Egyptian Journal of Radiology and Nuclear Medicine

RESEARCH Open Access

Can MRI predict lymphovascular invasion in breast cancer? A radiological-pathological observational insights

Nehal Magdy Settein[1*], Fatma Mohamed Sherif[1] and Eman Ashraf Saad[2]

Abstract

Aim of study To assess MRI features of invasive breast cancer in relation to lymphovascular invasion (LVI) and its clinicopathological associations.

Methods This retrospective study included 103 cases of pathologically proven breast cancer who had undergone preoperative MRI including conventional study, dynamic contrast-enhanced study (DCE) and diffusion-weighted imaging (DWI). Lesions were reviewed and described according to Breast Imaging Reporting and Data System (BIRADS) lexicon 2013 edition in addition to other MRI findings including: peritumoral edema, intratumoral high T2 signal intensity, tumor apparent diffusion coefficient (ADC) value, peritumoral ADC value, and peritumor–tumor ADC ratio. Histopathological and immunohistochemical analysis was done. Presence or absence of lymphovascular invasion (LVI) on postoperative histopathology was assessed. Statistical analyses were performed to identify significant MRI findings found with LVI as well as its clinicopathological associations.

Results Higher T-stage of the tumor ($p < 0.0001$), tumor histologic grade ($p < 0.0001$), molecular subtype (negative hormonal and positive HER2 status), high Ki-67 proliferation index ($p < 0.0001$), peritumoral edema ($p < 0.001$), intratumoral high T2 signal intensity ($p < 0.001$) were significantly associated with LVI. The tumor ADC value ($p = 0.034$), peritumoral ADC value ($p < 0.001$), and peritumor–tumor ADC ratio ($p < 0.001$) had significant correlation with LVI. Prediction of LVI can be made using cutoff value for peritumoral ADC (> 1.5) and peritumor/tumor ADC ratio (> 1.9) ($p < 0.001$).

Conclusions We found that lymphovascular invasion was more common in HER2-positive molecular subtypes and high-grade invasive tumors. T2-weighted imaging was helpful in detecting peritumoral edema and intratumoral high T2 signal which is strongly associated with lymphovascular invasion. Peritumoral ADC value and peritumor–tumor ADC ratio can be predictive MRI findings for LVI. This can impact management plans and patient prognosis especially in node-negative invasive breast cancer cases.

Keywords Invasive breast cancer, Magnetic resonance imaging (MRI), Lymphovascular invasion, Apparent diffusion coefficient (ADC)

Background

Breast cancer is considered one of the most prevalent malignancies in females worldwide [1]. Management of breast cancer is a complex process that requires multidisciplinary cooperation to achieve optimal outcome [2]. Breast cancer stage has been an essential factor to determine prognosis and management strategies; however, it is recently influenced by advanced pathological

*Correspondence:
Nehal Magdy Settein
nehalm60@mans.edu.eg
[1] Department of Diagnostic and Interventional Radiology, Faculty of Medicine, Mansoura University, Mansoura, Egypt
[2] Department of Pathology, Faculty of Medicine, Mansoura University, Mansoura, Egypt

tools that impact the treatment plan [3]. Pathologists can accurately identify the histopathological type, tumor histologic grade, and now the immunohistochemical biomarkers with the molecular subtype depending on estrogen receptor (ER), progesterone receptor (PR), human epidermal growth factor 2 (HER2), and proliferation index (Ki-67) [4].

Lymphovascular invasion (LVI) is the presence of malignant infiltrates in lymphatic and vascular spaces at perilesional region of an invasive cancer [5]. The presence of LVI increases the incidence of local recurrence, nodal and distant metastases [6, 7], and in addition, it acts as an independent factor in breast cancer patients with negative axillary lymphadenopathy [8]. Lymphovascular invasion (LVI) is currently evaluated on the postoperative specimen containing the excised malignant lesion with the surrounding breast tissue, which is challenging to evaluate in trucut biopsy as it is targeted to the malignant lesion only [9]. This highlights the value of preoperative imaging to show specific features related to LVI, which impacts the prognosis by predicting lymph node (LN) metastasis and consequently the treatment options [10].

Recent studies have focused on magnetic resonance imaging (MRI) findings in correlation with LVI [11–13]. Shi et al. [12] studied the margins of mass lesions, diffusion-weighted imaging signal, and dynamic curves in relation to LVI. Cheon et al. [13] included peritumoral edema in their analysis. However, some factors were discordant in these studies due to lack of more generalized data [11–13].

Diffusion-weighted imaging (DWI) is an MRI sequence depending on disparity of the water molecules Brownian motion within the tissue voxel [14]. The apparent diffusion coefficient (ADC) measures water diffusivity within the region of concern [14]. DWI and the ADC are powerful tools that can differentiate benign and malignant pathology [15]. Some previous studies revealed the benefit of ADC value as a reflection of tumor aggressiveness expressed as higher Ki-67 proliferation index (16]. Moreover, reduced ADC value within the tumor in the presence of LVI was reported in recent retrospective studies [17, 18]. This can be explained by the fact that the greater the cell turnover, the less the water molecules diffusivity in the tumor tissue and consequently lower ADC values [9]. Peritumor–tumor ADC ratio has been proposed to be a sensitive tool that could assess lymphedema associated with LVI, thus adding a value to peritumoral edema on T2-weighted imaging [9, 19].

However, some discordance in results of previous studies has been found that can be attributed to being retrospective. Another factor is the analysis of certain MRI parameters irrespective of other features in different imaging techniques (namely DWI). Thus, more comprehensive studies using various MRI techniques are needed to accurately define imaging features that could predict LVI in conjugation with other clinicopathological factors.

The aim of the current study was to determine the correlation between different MRI findings and lymphovascular invasion in patients with malignant invasive breast lesions and its clinicopathological associations. Identification of radiological features that could predict LVI could be beneficial to determine if additional treatment options are needed.

Materials and methods

Patients

This retrospective study included 103 cases of invasive breast cancer who underwent preoperative MRI from July 2024 to July 2025 in MRI unit at Radiology Department of Mansoura University Hospitals, followed by curative surgery either conservative breast surgery or mastectomy. Ethics approval was obtained by Mansoura Faculty of Medicine Institutional Research Board (approval number: R.25.07.3261). Informed consent was waived because this was a retrospective, anonymized study. Data collection and analysis were done through Picture Archiving and Communication System (PACS) in our institute. Inclusion criteria were newly diagnosed invasive breast cancer cases followed by surgery with histopathological and immunohistochemical evaluation of postoperative specimen, who underwent preoperative MRI with visible breast masses in their scan. Patients who received neoadjuvant chemotherapy and those with no provided immunohistochemical data were excluded from our study.

MRI acquisition

MRI was performed using commercially available 1.5 Tesla MRI machine (Philips Ingenia, Best, Netherlands) in prone position using a dedicated 16-channel breast coil. Conventional MRI study was done including a localizing sequence in sagittal plane followed by an axial TIWI without fat suppression using fast spin echo (FSE) (Repetition time (TR)/echo time (TE) 450 ms/14 ms, slice thickness 3 mm, field of view 300–360 mm). Axial T2-weighted sequence was obtained using FSE (Repetition time (TR)/echo time (TE) 2000 ms/80 ms, slice thickness 3 mm, field of view 300–360 mm) obtaining axial T2WI without fat suppression. Short TI inversion recovery (STIR) was performed (Repetition time (TR)/echo time (TE) 7000–9000 ms/70 ms, inversion time (TI) 150 ms, slice thickness 3–4 mm with inter-slice gap 1 mm, field of view 300–360 mm). Diffusion-weighted imaging (DWI) in axial plane was performed before contrast injection using single-shot echo-planar with

tri-directional diffusion gradients with b values at 0, 500, and 1000 mm^2/sec (slice thickness 4 mm, inter-slice gap 1 mm, 300–360 mm FOV, and 128 × 256 matrix) was used for all images. ADC maps were generated automatically using b values of 0, 500 and 1000 s/mm^2. Gadobenate dimeglumine (gadolinium) was injected at a dose of 0.1 mmol/kg of body weight to obtain contrast-enhanced images with axial T1-weighted (T1W) three-dimensional (3D) fat-suppressed fast spoiled gradient-echo sequence (Repetition time (TR)/echo time (TE) 4–8 ms/2 ms, flip angle 20–25 degrees, slice thickness 3 mm with no inter-slice gap, field of view 300–360 mm and matrix 384 × 384), fat suppression was done by applying fat-saturated pulse. This was performed one time before and five times after contrast injection each of them took about 1.15 min for acquisition of dynamic contrast-enhanced MRI (DCE-MRI) images.

Image analysis

The morphological criteria and enhancement of the lesions on MRI were assessed by a breast radiologist (with 9 years of experience) blinded to patients' pathological data. The largest diameter of the lesion in the early T1W images was measured. Breast Imaging Reporting and Data System (BIRADS) MRI lexicon [20] was used for lesion interpretation including mass and non-mass enhancement, and masses were described according to shape (oval, round, irregular), margin (circumscribed, irregular, spiculated), and internal enhancement characteristics (homogeneous, heterogeneous, rim enhancement). Non-mass enhancement was described according to distribution (focal, linear, segmental, regional, multiple regions, diffuse) and internal enhancement characteristics (homogeneous, heterogeneous, clumped, clustered ring). Tumor enhancement dynamics were evaluated visually as follows: type 1 curve (progressive enhancement pattern), type 2 curve (plateau pattern), and type 3 curve (washout pattern). Intratumoral high signal intensity on T2W images was evaluated by comparing it to signal intensity of normal breast parenchyma primarily on T2W image (in addition to STIR images), and interpreted as very high (when similar to water or vessels), high (when higher than normal parenchyma), and low (lower than normal parenchyma). Peritumoral edema was evaluated in T2W and STIR images and assigned as present when there was increased signal around the lesion. The ADC values of the tumor and peritumoral tissue were measured by ROIs placed on the ADC maps manually and calculated by MRI software. Axial ADC maps in the single section showing the maximum diameter of the tumor were chosen for placing ROI. An oval or round ROI as large as possible was placed inside the tumor on the basis of previous study revealing that the mean value of the largest round or oval ROI inside the tumor correlated with a Ki-67 index [16]. Multiple ROIs (at least three) were applied within the tumor. Cystic or necrotic areas were avoided while placing ROIs with reference to T2 and dynamic contrast-enhanced imaging. The lowest ADC value among the three mean tumor ADC values from multiple ROIs was accepted as tumor ADC value based on the inverse relationship between proliferation of tumor cells and ADC values [17]. For the peritumoral ADC value, ROIs were manually placed within 2 cm from the border between the tumor and the normal breast parenchyma in almost the same section of the tumor ADC measurement, taking almost same ROI size among cases. Three measurements at least were taken, and the maximum value among the three maximum peritumoral ADC values was accepted as peritumoral ADC value attributed to the presence of lymphedema with LVI [16].

The peritumor–tumor ADC ratio was calculated using the following formula [16]:

$$\text{Peritumoral}-\text{tumor ADC ratio} = \text{peritumoral maximum ADC value} / \text{tumor mean ADC value}$$

Pathological evaluation

Pathological reports from postoperative surgical specimen (including excisional biopsy, conservative breast surgery and mastectomy) were reviewed by a breast pathologist (with 10 years of experience). Histological analysis was done including tumor histologic type, histologic grading and invasive tumor size. Immunohistochemical staining was performed to assess status of ER, PR, HER2, and Ki-67 index. ER and PR expression were calculated using the Allred scoring system and were considered as positive for ER or PR with a total Allred score > 2 [21]. The intensity of HER2 staining was scored as 0, 1+, 2+, or 3+. Masses having score of 3+were assigned as HER2-positive, while those with a score of 0 or 1+were considered negative. Score 2+was described as equivocal which needed another testing with fluorescence in situ hybridization (FISH). Ki-67 expression was recorded as the percentage of tumor epithelial cells evaluated on immunohistochemical assay where Ki-67 level of 14% or less was considered as low Ki-67 index, while Ki-67 level higher than 14% was considered as high Ki-67 index. Molecular subtyping was done for malignant breast lesions. LVI was evaluated by hematoxylin-and-eosin-stained sections when malignant cells are

present in an endothelial-lined space in the perilesional parenchyma.

Statistical analysis

Data were entered and analyzed using IBM SPSS software (IBM Corp. Released 2020. IBM SPSS Statistics for Windows, Version 27.0. Armonk, NY: IBM Corp), and MedCalc® Statistical Software version 23.1.5 (MedCalc Software Ltd, Ostend, Belgium; 2025). Diagnostic performance was analyzed using an online calculator [https://www.dcode.fr/confusion-matrix]. *Qualitative data* were expressed as count (N) and percentage (%). *Quantitative data* were initially tested for normality using Shapiro–Wilk's test (normally distributed data has $p > 0.050$) and Q–Q plots. Detection of significant outliers was done by inspecting boxplots. Quantitative data were expressed as median, Q1 (25th percentile), and Q3 (75th percentile). The Chi-square test, Fisher's exact test, and Fisher–Freeman–Halton exact test were used to examine the association between two categorical variables when appropriate. Comparison of a quantitative variable between two groups was done by Mann–Whitney U test. Binary logistic regression (univariable and multivariable) was used to ascertain the effects of predictor variables on the likelihood that participants will exhibit lymphovascular invasion (LVI). For simplicity and convenience, a cutoff value for each quantitative predictor variable was created by ROC curve analysis. For any of the tests used, results were considered as statistically significant if p value ≤ 0.050. Graphical representation of the results was performed using the relevant charts if required.

Results

Patients:

The mean age within the study was 47 years (range, 27–69 years). Most of the lesions were invasive duct carcinoma (94/103, 91.3%). The commonest molecular subtype was luminal B (57/103, 55.3%), and moderate differentiation was the most common histologic grade (51/103, 59.2%). Histopathological examination revealed patients with ($n = 33$) and without LVI ($n = 70$) among the 103 lesions.

LVI vs. clinicopathological features

Studying LVI in relation to clinicopathological data (Table 1), there was a statistically significant difference in T-stage, histologic grade, molecular subtype, hormone status, HER2 status, and Ki-67 status in correlation with LVI. Regarding T-stage, the test of significance is the Chi-square test, multiple z-tests were conducted and revealed that T1 tumors were more in negative LVI group while T3 tumors were more in positive LVI group. Regarding histological grade, the test of significance is Fisher–Freeman–Halton exact test, so dummy variables were created to perform multiple 2 × 2 Fisher exact tests which revealed that grades I and II were more with negative LVI while grade III was more with positive LVI. Regarding molecular subtype, the test of significance is Fisher–Freeman–Halton exact test, so, dummy variables were created to perform multiple 2 × 2 Fisher exact tests which revealed that luminal A was more in negative LVI cases while HER2-enriched was more in positive LVI ones. Both ER- and PR-positive tumors were more in negative LVI group while positive HER2 and high Ki-67 tumors were found more in positive LVI group.

Table 1 Clinicopathological characteristics of patients according to lymphovascular invasion status

Characteristic	Lymphovascular invasion (LVI)				Sig
	Negative		Positive		
	N	%	N	%	
Histologic type Invasive duct carcinoma Invasive lobular carcinoma	64 6	91.4 8.6	30 3	90.9 9.1	1.000
Histologic grade Low Moderate High	15 53 2	21.4 75.7 2.9	0 8 25	0 24.2 75.8	< .001
Molecular subtype Luminal A Luminal B HER2-enriched Triple negative	32 35 3 0	45.7 50 4.3 0	0 22 8 3	0 66.7 24.2 9.1	< .001
ER status Positive Negative	67 3	95.7 4.3	22 11	66.7 33.3	< .001
PR status Positive Negative	62 8	88.6 11.4	20 13	60.6 39.4	.001
HER2 status Positive Negative	17 53	24.3 75.7	16 17	48.5 51.5	.014
Ki-67 status Low (< 15%) High (> 15%)	54 16	77.1 22.9	1 32	3 97	< .001
T-stage T1 T2 T3	18 a 47 a 5 a	25.7 67.1 7.1	2 b 19 a 12 b	6.1 57.6 36.4	< .001

Notes: Sig. = statistical significance (p value). Categorical data are N (%) and are compared by Chi-square test, Fisher's Exact Test, or Fisher–Freeman–Halton exact test when appropriate. Multiple z-tests are denoted by small letters (different letters = statistically significant difference)

LVI vs. MRI features

In this study, the mass and non-mass enhancement characteristics on DCE-MRI as well as the time signal intensity curve data showed no significant correlation with

Table 2 MRI features and lymphovascular invasion status

Characteristic	Lymphovascular invasion (LVI)				Sig
	Negative		Positive		
	N	%	N	%	
Amount of fibroglandular tissue (FGT) Scattered Heterogeneous Extreme	6 62 2	8.6 88.6 2.9	8 24 1	24.2 72.7 3	.089
Background parenchymal enhancement (BPE) Minimal Mild Moderate Marked	2 47 20 1	2.9 67.1 28.6 1.4	5 22 5 1	15.2 66.7 15.2 3	.056
Lesion morphology Mass NME	49 21	70 30	22 11	66.7 33.3	.733
Mass shape Round Irregular	3 46	6.1 93.3	4 18	18.2 81.8	.192
Mass margin Circumscribed Irregular Spiculated	1 38 10	2 77.6 20.4	3 15 4	13.6 68.2 18.2	.176
Mass internal enhancement Heterogeneous Rim	45 4	91.8 8.2	20 2	90.9 9.1	1.000
NME distribution Linear Segmental Regional	1 16 4	4.8 76.2 19	0 5 6	0 45.5 54.5	.106
NME internal enhancement Heterogeneous Clumped	18 3	85.7 14.3	9 2	81.8 18.2	1.000
Kinetic curve type Plateau Washout	36 34	51.5 48.6	12 21	36.4 63.6	.153
Peritumoral edema	4	5.7	28	84.8	< .001
Intratumoral high T2 signal	2	2.9	17	51.5	< .001
Tumor ADC value > 0.8 ≤ 0.8	43 27	61.4 38.6	14 19	42.4 57.6	.070
Peritumoral ADC value ≤ 1.5 > 1.5	56 14	80 20	7 26	21.2 78.8	< .001
Peritumor/Tumor ADC ratio ≤ 1.9 > 1.9	67 3	95.7 4.3	8 25	24.2 75.8	< .001
	Median	**Q1-Q3**	**Median**	**Q1-Q3**	**Sig**
Tumor ADC value	0.9	0.8–1.0	0.8	0.7–0.9	.034
Peritumoral ADC value	1.3	1.2–1.5	1.9	1.6–2.3	< .001
Peritumor/Tumor ADC ratio	1.5	1.4–1.7	2.3	1.9–2.7	< .001

Notes: Sig. = statistical significance (p value). Categorical data are N (%) and compared by Chi-square test, Fisher's Exact Test, or Fisher–Freeman–Halton Exact Test when appropriate. Multiple z-tests are small letters (different letters = statistically significant difference). Quantitative data are median and Q1 [25th percentile]–Q3 [75th percentile] and compared by Mann–Whitney U test

LVI; however, MRI findings on T2WI including peritumoral edema and intratumoral high T2 signal had significant associations with LVI (Table 2). For the positive LVI group there was peritumoral edema (Fig. 1), while in the negative LVI group there was no peritumoral edema

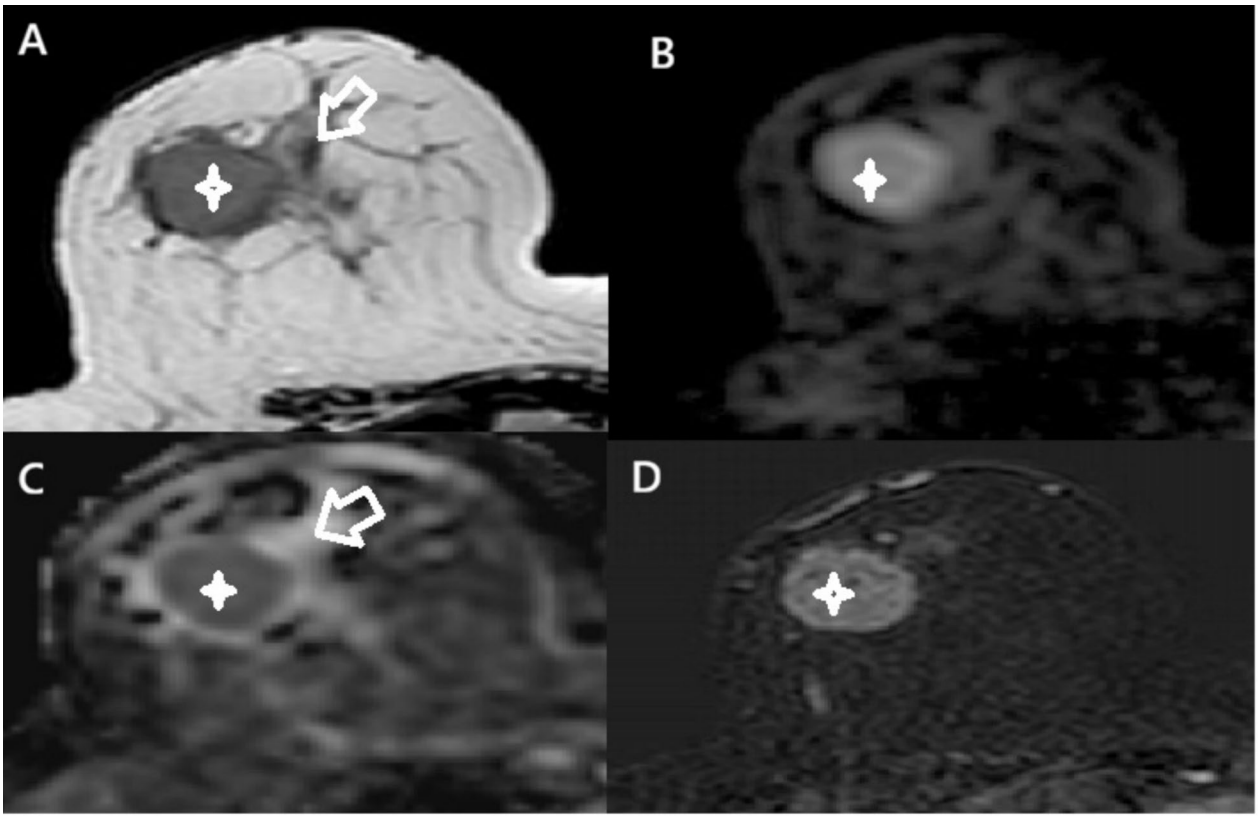

Fig. 1 Images of a 37-year-old woman with invasive ductal carcinoma and a lymphovascular invasion. **A** Axial T2-weighted image shows a 4.2 cm mass in her right breast. Intratumoral T2 high signal (asterisk) and peritumoral edema (arrow) are noted. **B** High signal of the lesion (asterisk) is shown in axial diffusion-weighted image (b value = 1000 s/mm^2). **C** Axial ADC map shows low signal intensity of the lesion (asterisk) denoting diffusion restriction and higher signal intensity of the region surrounding the mass (arrow). The tumor ADC value was 0.7 ($\times 10^{-3}$ mm^2/s), the peritumoral ADC value was 2.3 ($\times 10^{-3}$ mm^2/s). The peritumor–tumor ADC ratio was 3.28. **D** Axial contrast-enhanced T1-weighted image demonstrating a round, partially circumscribed heterogeneously enhancing mass in her right breast (asterisk). This patient underwent modified radical mastectomy of her right breast. The histopathological features of this mass were poorly differentiated, triple-negative breast cancer, ER-, PR-, HER2- and Ki-67 high (70%). Tumor size at final pathologic report was 5.5 cm

(Fig. 2). A high intratumoral T2W signal was more common in positive LVI group (Fig. 1).

In terms of LVI and DWI (Table 3), peritumoral ADC value > 1.5 and peritumor/Tumor ADC ratio > 1.9 were found with positive LVI. Regarding numerical data, lower tumor ADC value and higher peritumoral ADC value and peritumor/Tumor ADC ratio were associated with positive LVI. The AUC for the tumor ADC value was 0.626 (Fig. 3), the peritumor ADC value was 0.853 (Fig. 4), and for the peritumor–tumor ADC ratio was 0.842 (Fig. 5). Tumor ADC value ($\times 10^{-3}$ mm^2/s) ≤ 0.8, Peritumoral ADC value ($\times 10^{-3}$ mm^2/s) > 1.5, and Peritumor/tumor ADC ratio > 1.9 were statistically significant diagnostic tests for LVI, with an overall accuracy of 60.2, 79.6, and 89.3, respectively.

The results of binary logistic regression (Table 4) which was run to ascertain the effects of tumor ADC value ≤ 0.8, peritumoral ADC value > 1.5, peritumor/tumor ADC ratio > 1.9, peritumoral edema, intratumoral high T2 signal intensity, and age < 42 years on the likelihood that participants will exhibit LVI. These predictors were compared to tumor ADC value > 0.8, peritumoral ADC value ≤ 1.5, peritumor/tumor ADC ratio ≤ 1.9, absence of peritumoral edema, absence of intratumoral high T2 signal intensity, and age ≥ 42 years as reference categories, respectively.

On univariable analysis, five variables were statistically significant which are peritumoral ADC value > 1.5, peritumor/tumor ADC ratio > 1.9, peritumoral edema, intratumoral high T2 signal intensity, and age < 42 years. These predictor variables were entered in the multivariable logistic regression model.

On multivariable analysis, the model was statistically significant (χ^2 [5] = 85.11, $p < 0.001$). The model correctly classified 92.2% of cases with 84.8% sensitivity, 95.7% specificity, 90.3% PPV, and 93.1% NPV.

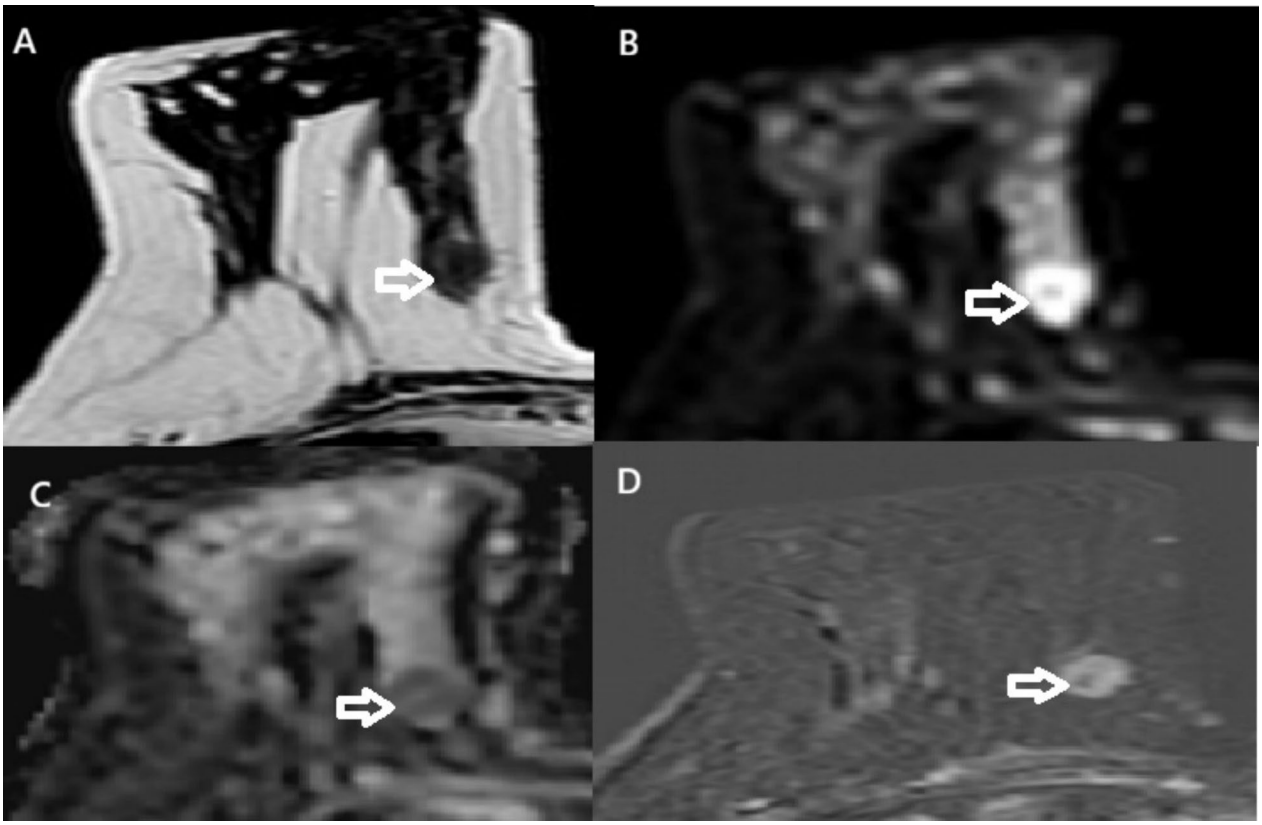

Fig. 2 Images of a 61-year-old woman with invasive ductal carcinoma without lymphovascular invasion. **A** Axial T2-weighted image shows a 2.3 cm mass in her right breast with low-to-intermediate T2 high signal and high STIR signal (arrow). **B** Axial diffusion-weighted image (b value = 1000 s/mm^2) showing high signal intensity of mass (arrow). **C** Axial ADC map shows low signal intensity of the lesion (arrow), denoting diffusion restriction. The region surrounding the mass is isointense compared to other regions within the breast tissue. The tumor ADC value was 0.8 ($\times 10^{-3}$ mm^2/s), peritumoral ADC value was 1.4, peritumor–tumor ADC ratio was 1.75. **D** Axial contrast-enhanced T1-weighted image demonstrating an irregular speculated mass with heterogeneous enhancement in her right breast. This patient underwent conservative breast surgery. The histopathological features of this mass were moderately differentiated luminal A breast cancer, ER+, PR+, HER2-, and Ki-67 high (20%). Tumor size at final pathologic report was 2.5 cm

Discussion

Lymphovascular invasion (LVI) is considered as a predictive factor for axillary lymphadenopathy and distant metastasis. Local and systemic recurrence is associated with LVI especially in cases with negative nodal status [8].

Recent studies were concerned with the relation between LVI and various clinicopathological prognostic factors of breast cancer, including immunohistochemical subtype, tumor size, axillary lymph nodes status, and histological grade [22]. In the current study, we found a significant correlation between LVI and T-stage of the tumor, histologic grade, hormone receptor status and Ki-67 status. Although these results were discordant with Cheon et al. [13] who found no significant correlation of these factors with LVI, a meta-analysis done by Shen et al. [22] found that the combined results of included studies indicated that LVI could predict worse outcome for invasive breast cancer as it is correlated with the tumor size, regional lymph node involvement and histological grade. Higher Ki-67 level in LVI-positive cases was found by Mounir et al. [23] which was consistent with our results, reflecting the aggressiveness of these tumors.

Regarding DCE-MRI findings of breast cancer in relation to LVI, some studies have reported associations between LVI and certain BIRADS descriptors [19], yet in this study we found no correlation between MRI BIRADS descriptors for mass or non-mass enhancement lesions and LVI. This was in line with Cheon et al. [13], who described that MRI features from BIRADS lexicon did not reveal statistically significant association with LVI, except for regional enhancement in non-mass enhancement lesions, which was more frequently found in cases with positive LVI than in negative LVI cases.

In terms of LVI and MRI features on T2WI, peritumoral edema and high intratumoral T2 signal on MRI

Table 3 ADC parameters in relation to lymphovascular invasion status

Characteristic	Lymphovascular invasion (LVI)				Sig
	Negative		Positive		
	N	%	N	%	
Tumor ADC value					.070
> 0.8	43	61.4	14	42.4	
≤ 0.8	27	38.6	19	57.6	
Peritumoral ADC value					< .001
≤ 1.5	56	80	7	21.2	
> 1.5	14	20	26	78.8	
Peritumor/Tumor ADC ratio					< .001
≤ 1.9	67	95.7	8	24.2	
> 1.9	3	4.3	25	75.8	
	Median	**Q1-Q3**	**Median**	**Q1-Q3**	**Sig**
Tumor ADC value	0.9	0.8–1.0	0.8	0.7–0.9	.034
Peritumoral ADC value	1.3	1.2–1.5	1.9	1.6–2.3	< .001
Peritumor/Tumor ADC ratio	1.5	1.4–1.7	2.3	1.9–2.7	< .001

Sig. = statistical significance (*p* value). Categorical data are N (%) and compared by Chi-square test, Fisher's Exact Test, or Fisher–Freeman–Halton Exact Test when appropriate. Multiple z-tests are small letters (different letters = statistically significant difference). Quantitative data are median and Q1 [25th percentile]–Q3 [75th percentile] and compared by Mann–Whitney U test

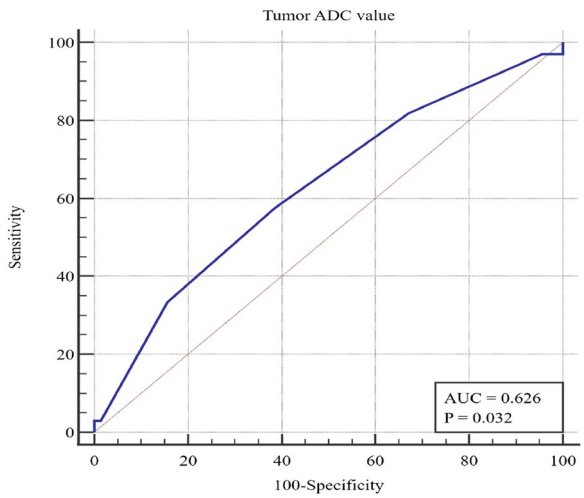

Fig. 3 ROC curve for Tumor ADC value in discriminating positive from negative LVI

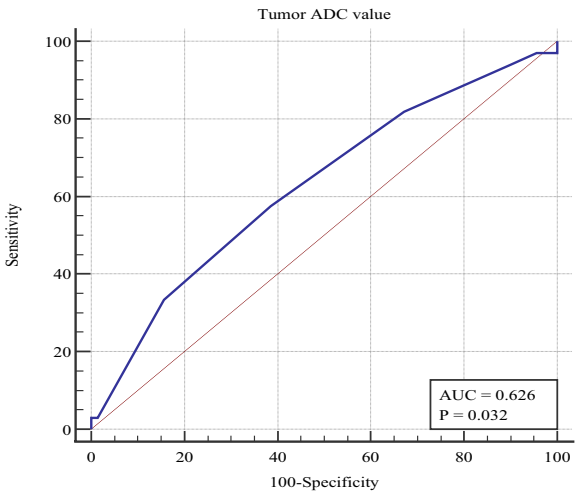

Fig. 4 ROC curve for Peritumor ADC value in discriminating positive from negative LVI

were believed to be prognostic factors associated with reduced survival due to their association with LVI [24, 25]. Peritumoral edema occurs due to higher permeability of vascular spaces and release of peritumoral cytokines [26]. Intratumoral high T2 signal intensity reflects rapid turnover of neoplastic cells that outgrow their vascular supply, resulting in hypoxia and necrosis mainly affecting the central area of the tumor [27]. In a study by Dietzel et al. [28], central high intratumoral T2 SI within a T2-hypointense breast mass is linked to tumor aggressiveness that has a high histologic grade and larger tumor size, with high Ki-67 value [29]. Intratumoral high T2 signal and peritumoral edema were found to be associated with LVI in some recent studies [13, 30]. Our data showed that intratumoral high T2 signal on T2WI was detected in cases with positive LVI. Peritumoral edema was present in the positive LVI group more than in the negative LVI group. Similarly, a study by Pamela Sung

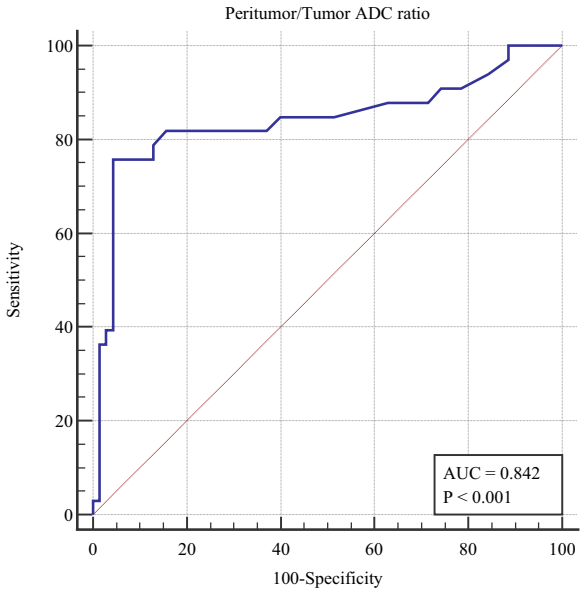

Fig. 5 ROC curve for Peritumor/Tumor ADC ratio in discriminating positive from negative LVI

et al. [31] observed that LVI was more frequently found in edema-positive group than in edema-negative group (57.9% vs. 12.6%, $p < 0.001$). On the contrary, Choi et al. [19] reported no significant correlation between LVI and the aforementioned T2 findings. This may be attributed to their selection of node-negative patients only.

Many studies have reported that ADC values had significant correlations with LVI [17, 32, 33]. Our results were in agreement with a retrospective cohort study that reported reduced ADC values in cases with LVI than those without [34], and also consistent with conclusions of another previous study that tumor ADC value, peritumor–tumor ADC ratio, lesion size, Ki-67 index, and axillary lymphadenopathy showed statistically significant difference in relation to LVI [16]. Previous reports suggested correlations between the tumor ADC value and markers of lesion aggressiveness, namely Ki-67 index [35, 36], which is also associated with vascular and lymphatic invasion [37]. We were in agreement with this in our study, defining the tumor ADC value as the lowest of the mean ADC values of the tumor.

In the current study, peritumoral ADC values showed a significant difference in relation to LVI, where LVI-positive cases showed higher peritumoral ADC values. Choosing the highest of peritumoral maximum ADC values as the peritumoral ADC value was based on the presence of peritumoral lymphedema caused by LVI, this was concordant with Mori et al. [16] who also reported a significant difference in peritumoral ADC value in correlation to LVI. When reviewing statistical significance of tumor ADC value in comparison with peritumoral ADC values in relation to LVI, it was found that the tumor ADC value demonstrated relatively moderate discriminatory performance compared with the peritumoral ADC value. This could be attributed to the heterogeneity of the tumor cells on histological as well as immunohistochemical basis, resulting in variations in ADC values which is sensitive to both pathological profiles. Okuma et al. [38] described that high peritumor/tumor ADC ratio reflects lesion aggressiveness in terms of size, histologic grade and lymph node involvement. They highlighted the value of peritumoral–tumoral ADC ratio as a predictive factor of LVI and peritumoral edema which is associated with disease recurrence [38]. It was observed in this study that a higher peritumor/tumor ADC ratio was significantly associated with LVI. Aggressive breast cancers were found to have higher peritumoral ADC values, reflecting peritumoral edema. Accordingly, peritumoral ADC might be used as an objective tool to detect early edema before appearance of its morphological findings on DCE-MRI [39].

Table 4 Predictors of LVI

Predictor	Univariable				Multivariable			
	Sig	COR	95% CI		Sig	AOR	95% CI	
			Lower	Upper			Lower	Upper
Tumor ADC value ≤ 0.8	.073	2.16	0.93	5.01				
Peritumoral ADC value > 1.5	< .001	14.86	5.36	41.18	.569	.490	.042	5.682
Peritumor/Tumor ADC ratio > 1.9	< .001	69.79	17.1	284.2	.031	18.486	1.315	259.793
Peritumoral edema	< .001	92.40	23.1	269.9	< .001	29.166	5.098	166.864
Intratumoral high T2 signal intensity	< .001	36.13	7.57	172.4	.127	7.361	.568	95.321
Age < 42 years	.007	3.31	1.38	7.94	.327	2.355	.425	13.059

Notes: Sig. = statistical significance (*p* value). COR = crude odds ratio. AOR = adjusted odds ratio. CI = confidence interval

This study had some limitations; one of them was being retrospective one reviewed by single radiologist. The results would be more convincing if the MRI data could be reviewed by more than one radiologist. This was attributed to the need of experienced breast radiologist in breast MRI interpretation for assessment of the studied variables, which is considered challenging in a single-institute study. One more drawback to the single-institute study is the small sample size, which impacted on the validity of some results especially in multivariate regression model; findings would benefit from validation in larger or multi-center cohorts in future studies. Another limitation was the reproducibility of drawing ROIs for ADC measurements especially in small tumors.

Conclusions

Some MRI findings can be used as predictors for LVI along with other clinicopathological associations. This can impact management plans and patient prognosis especially in invasive breast cancer cases with negative nodal disease.

Abbreviations

MRI	Magnetic resonance imaging
LVI	Lymphovascular invasion
DWI	Diffusion-weighted images
DCE	Dynamic contrast enhanced
BIRADS	Breast Imaging Reporting and Data System
ADC	Apparent diffusion coefficient
ER	Estrogen receptor
PR	Progesterone receptor
HER2	Human epidermal growth factor 2
PACS	Picture archiving and communication system
FSE	Fast spin echo
TR	Repetition time
TE	Echo time
STIR	Short TI inversion recovery
TI	Inversion time
ROI	Region of interest
FISH	Fluorescence in situ hybridization
PPV	Positive predictive value
NPV	Negative predictive value

Acknowledgements
Not applicable.

Author contributions
NM Settein analyzed and interpreted the breast MRI findings and reviewed the patient's clinical data. EA Saad performed the histological examination of the breast specimens and FM Sherif was a major contributor in writing the manuscript. All authors read and approved the final manuscript.

Funding
None.

Data availability
The datasets used and/or analysed during the current study are available from the corresponding author on reasonable request.

Declarations

Ethics approval and consent to participate
This study was approved by Mansoura Faculty of Medicine Institutional Research Board (approval number: R.25.07.3261). Informed consent was waived because this was a retrospective, anonymized study.

Consent for publication
Not applicable.

Competing interests
The authors declare no competing interests.

Received: 23 December 2025 Accepted: 27 April 2026
Published online: 08 May 2026

References:

1. Feng Y, Spezia M, Huang S, Yuan C, Zeng Z, Zhang L, Ji X, Liu W, Huang B, Luo W, Liu B, Lei Y, Du S, Vuppalapati A, Luu HH, Haydon RC, He T-C, Ren G (2018) Breast cancer development and progression: risk factors, cancer stem cells, signaling pathways, genomics, and molecular pathogenesis. Genes Dis 5(2):77–106
2. Chatterjee A, Erban JK (2017) Neoadjuvant therapy for treatment of breast cancer: the way forward, or simply a convenient option for patients? Gland Surg 6(1):119
3. Alili C, Pages E, Doyon FC, Perrochia H, Millet I, Taourel P (2014) Correlation between MR imaging–prognosis factors and molecular classification of breast cancers. Diagn Interv Imaging 95(2):235–242
4. Zubair M, Wang S, Ali N (2021) Advanced approaches to breast cancer classification and diagnosis. Front Pharmacol 11:632079
5. Ryu YJ, Kang SJ, Cho JS, Yoon JH, Park MH (2018) Lymphovascular invasion can be better than pathologic complete response to predict prognosis in breast cancer treated with neoadjuvant chemotherapy. Medicine 97(30):e11647
6. Liao GS, Hsu HM, Chu CH, Hong ZJ, Fu CY, Chou YC, Golshan M, Dai M-S, Chen T-W, De-Chian C, Tsai W-C, Pan C-W, Hsu K-F, Kao E-N, Hsu Y-C, Chang T-H, Yu JC (2018) Prognostic role of lymphovascular invasion and lymph node status among breast cancer subtypes. J Med Sci 38(2):54–61
7. Zhu Z, Wang W, Lin F, Jordan T, Li G, Silverman S, Wong GK (2019) Genome profiles of lymphovascular breast cancer cells reveal multiple clonally differentiated outcomes with multi-regional LCM and G&T-seq
8. Matsuda N, Hayashi N, Ohde S, Yagata H, Kajiura Y, Yoshida A, Yamauchi H (2014) A nomogram for predicting locoregional recurrence in primary breast cancer patients who received breast-conserving surgery after neoadjuvant chemotherapy. J Surg Oncol 109(8):764–769
9. Igarashi T, Furube H, Ashida H, Ojiri H (2018) Breast MRI for prediction of lymphovascular invasion in breast cancer patients with clinically negative axillary lymph nodes. Eur J Radiol 107:111–118
10. Kuhn E, Gambini D, Despini L, Asnaghi D, Runza L, Ferrero S (2023) Updates on lymphovascular invasion in breast cancer. Biomedicines 11(3):968
11 Ouyang FS, Guo BL, Huang XY, Ouyang LZ, Zhou CR, Zhang R, Hu QG (2019) A nomogram for individual prediction of vascular invasion in primary breast cancer. Eur J Radiol 110:30–38
12. Ni-jia-ti MY, Ai-hai-ti DL, Huo-jia AS, Wu-mai-er PL, A-bu-li-zi AB, Shi Y, Rou-zi NE, Su WJ, Dai GZ, Da-mo-la MH (2020) Development of a risk-stratification scoring system for predicting lymphovascular invasion in breast cancer. BMC Cancer 20(1):94
13 Cheon H, Kim HJ, Lee SM, Cho SH, Shin KM, Kim GC, Kim WH (2017) Preoperative MRI features associated with lymphovascular invasion in node-negative invasive breast cancer: a propensity-matched analysis. J Magn Reson Imaging 46(4):1037–1044
14. Partridge SC, Nissan N, Rahbar H, Kitsch AE, Sigmund EE (2017) Diffusion-weighted breast MRI: clinical applications and emerging techniques. J Magn Reson Imaging 45(2):337–355

15 Fusco R, Sansone M, Filice S, Granata V, Catalano O, Amato DM, Petrillo A (2015) Integration of DCE-MRI and DW-MRI quantitative parameters for breast lesion classification. BioMed Res Int 2015(1):237863
16. Mori N, Mugikura S, Takasawa C, Miyashita M, Shimauchi A, Ota H, Takahashi S (2016) Peritumoral apparent diffusion coefficients for prediction of lymphovascular invasion in clinically node-negative invasive breast cancer. Eur Radiol 26(2):331–339
17. Durando M, Gennaro L, Cho GY, Giri DD, Gnanasigamani MM, Patil S, Sutton EJ, Deasy JO, Morris EA, Thakur SB (2016) Quantitative apparent diffusion coefficient measurement obtained by 3.0 Tesla MRI as a potential noninvasive marker of tumor aggressiveness in breast cancer. Eur J Radiol 85(9):1651–1658
18. Abe H, Schmidt RA, Kulkarni K, Sennett CA, Mueller JS, Newstead GM (2009) Axillary lymph nodes suspicious for breast cancer metastasis: sampling with US-guided 14-gauge core-needle biopsy—clinical experience in 100 patients. Radiology 250(1):41–49
19. Choi BB (2021) Dynamic contrast enhanced-MRI and diffusion-weighted image as predictors of lymphovascular invasion in node-negative invasive breast cancer. World J Surg Oncol 19(1):76
20. Sickles EA, Appleton CM, Burnside ES, Gavenonis SC (2013) Breast imaging reporting and data system (BI-RADS) Atlas-Ultrasound 5th edn. In: American College of Radiology BI-RADS-Atlas
21. Allred DC, Harvey JM, Berardo M, Clark GM (1998) Prognostic and predictive factors in breast cancer by immunohistochemical analysis. Mod Pathol 11(2):155–168
22. Shen SD, Zhong SZ, Wang CZ, Huang WH (2015) Correlation of lymphovascular invasion with clinicopathological factors in invasive breast cancer: a meta-analysis. Int J Clin Exp Med 8(10):17789
23. Mounir AM, Shokeir FA, AbdElraouf GH (2025) Breast imaging: correlation between axillary lymph nodes apparent diffusion coefficient and pathological lymphovascular invasion in patients with invasive breast cancer. Eur J Breast Health 21(2):141
24. Uematsu T, Kasami M, Yuen S (2009) Triple-negative breast cancer: correlation between MR imaging and pathologic findings. Radiology 250(3):638–647
25. Uematsu T, Kasami M, Watanabe J (2014) Is evaluation of the presence of prepectoral edema on T2-weighted with fat-suppression 3 T breast MRI a simple and readily available noninvasive technique for estimation of prognosis in patients with breast cancer? Breast Cancer 21(6):684–692
26 Baltzer PA, Yang F, Dietzel M, Herzog A, Simon A, Vag T, Kaiser WA (2010) Sensitivity and specificity of unilateral edema on T2w-TSE sequences in MR-mammography considering 974 histologically verified lesions. Breast J 16(3):233–239
27. Jing X, Yang F, Shao C, Wei K, Xie M, Shen H, Shu Y (2019) Role of hypoxia in cancer therapy by regulating the tumor microenvironment. Mol Cancer 18(1):157
28. Dietzel M, Baltzer PA, Vag T, Herzog A, Gajda M, Camara O, Kaiser WA (2010) The necrosis sign in magnetic resonance-mammography: diagnostic accuracy in 1,084 histologically verified breast lesions. Breast J 16(6):603–608
29 Yuen S, Monzawa S, Yanai S, Matsumoto H, Yata Y, Ichinose Y, Yamagami K (2020) The association between MRI findings and breast cancer subtypes: focused on the combination patterns on diffusion-weighted and T2-weighted images. Breast Cancer 27(5):1029–1037
30. Bae MS, Shin SU, Ryu HS, Han W, Im SA, Park IA, Moon WK (2016) Pretreatment MR imaging features of triple-negative breast cancer: association with response to neoadjuvant chemotherapy and recurrence-free survival. Radiology 281(2):392–400
31. Sung P, Lee JY, Cheun JH, Choi IS, Park JH, Park JH, Hwang KT (2023) Prognostic implication of focal breast edema on preoperative breast magnetic resonance imaging in breast Cancer patients. J Breast Cancer 26(5):479
32. Karan B, Pourbagher A, Torun N (2016) Diffusion-weighted imaging and 18F-fluorodeoxyglucose positron emission tomography/computed tomography in breast cancer: correlation of the apparent diffusion coefficient and maximum standardized uptake values with prognostic factors. J Magn Reson Imaging 43(6):1434–1444
33. Yang W, Qiang JW, Tian HP, Chen B, Wang AJ, Zhao JG (2017) Minimum apparent diffusion coefficient for predicting lymphovascular invasion in invasive cervical cancer. J Magn Reson Imaging 45(6):1771–1779
34. Mori N, Ota H, Mugikura S, Takasawa C, Ishida T, Watanabe G, Tada H, Watanabe M, Takase K, Takahashi S (2015) Luminal-type breast cancer: correlation of apparent diffusion coefficients with the Ki-67 labeling index. Radiology 274(1):66–73
35. Shin HJ, Kim SH, Lee HJ, Gong G, Baek S, Chae EY, Choi WJ, Cha JH, Kim HH (2016) Tumor apparent diffusion coefficient as an imaging biomarker to predict tumor aggressiveness in patients with estrogen-receptor-positive breast cancer. NMR Biomed 29(8):1070–1078
36. Jacquemier J, Charafe-Jauffret E, Monville F, Esterni B, Extra JM, Houvenaeghel G, Birnbaum D (2009) Association of GATA3, P53, Ki67 status and vascular peritumoral invasion are strongly prognostic in luminal breast cancer. Breast Cancer Res 11(2):R23
37. Cheon H, Kim HJ, Kim TH, Ryeom HK, Lee J, Kim GC, Yuk J-S, Kim WH (2018) Invasive breast cancer: prognostic value of peritumoral edema identified at preoperative MR imaging. Radiology 287(1):68–75
38. Okuma H, Sudah M, Kettunen T, Niukkanen A, Sutela A, Masarwah A, Kosma V-M, Auvinen P, Mannermaa A, Vanninen R (2020) Peritumor to tumor apparent diffusion coefficient ratio is associated with biologically more aggressive breast cancer features and correlates with the prognostication tools. PLoS ONE 15(6):e0235278
39. Sung JS, Jochelson MS, Brennan S, Joo S, Wen YH, Moskowitz C, Zheng J, Dershaw DD, Morris EA (2013) MR imaging features of triple-negative breast cancers. Breast J 19(6):643–649

Publisher's Note